NeuroImage: Clinical 39 (2023) 103505

Contents lists available at ScienceDirect

NeuroImage: Clinical

journal homepage: www.elsevier.com/locate/ynicl

Structural and microstructural neuroimaging signature of *C9orf72*-associated ALS: A multiparametric MRI study

Maximilian Wiesenfarth [a], Hans-Jürgen Huppertz [b], Johannes Dorst [a,c], Dorothée Lulé [a], Albert C. Ludolph [a,c], Hans-Peter Müller [a,1], Jan Kassubek [a,c,1,*]

[a] *Department of Neurology, University Hospital Ulm, Ulm, Germany*
[b] *Swiss Epilepsy Clinic, Klinik Lengg, Zürich, Switzerland*
[c] *German Centre of Neurodegenerative Diseases (DZNE), Ulm, Germany*

A R T I C L E I N F O

Keywords:
Diffusion tensor imaging
Atlas-based volumetry
Amyotrophic lateral sclerosis
C9orf72 expansion
Magnetic resonance imaging
Motor neuron disease

A B S T R A C T

Background: ALS patients with hexanucleotide expansion in *C9orf72* are characterized by a specific clinical phenotype, including more aggressive disease course and cognitive decline. Computerized multiparametric MRI with gray matter volumetry and diffusion tensor imaging (DTI) to analyze white matter structural connectivity is a potential *in vivo* biomarker.

Objective: The objective of this study was to develop a multiparametric MRI signature in a large cohort of ALS patients with *C9orf72* mutations. The aim was to investigate how morphological features of *C9orf72*-associated ALS differ in structural MRI and DTI compared to healthy controls and ALS patients without *C9orf72* mutations.

Methods: Atlas-based volumetry (ABV) and whole brain-based DTI-based analyses were performed in a cohort of $n = 51$ ALS patients with *C9orf72* mutations and compared with both $n = 51$ matched healthy controls and $n = 51$ *C9orf72* negative ALS patients, respectively. Subsequently, Spearman correlation analysis of *C9orf72* ALS patients' data with clinical parameters (age of onset, sex, ALS-FRS-R, progression rate, survival) as well as ECAS and p-NfH in CSF was performed.

Results: The whole brain voxel-by-voxel comparison of fractional anisotropy (FA) maps between *C9orf72* ALS patients and controls showed significant bilateral alterations in axonal structures of the white matter at group level, primarily along the corticospinal tracts and in fibers projecting to the frontal lobes. For the frontal lobes, these alterations were also significant between *C9orf72* positive and *C9orf72* negative ALS patients. In ABV, patients with *C9orf72* mutations showed lower volumes of the frontal, temporal, and parietal lobe, with the lowest values in the gray matter of the superior frontal and the precentral gyrus, but also in hippocampi and amygdala. Compared to *C9orf72* negative ALS, the differences were shown to be significant for cerebral gray matter ($p = 0.04$), especially in the frontal ($p = 0.01$) and parietal lobe ($p = 0.01$), and in the thalamus ($p = 0.004$). A correlation analysis between ECAS and averaged regional FA values revealed significant correlations between cognitive performance in ECAS and frontal association fibers. Lower FA values in the frontal lobes were associated with worse performance in all cognitive domains measured (language, verbal fluency, executive functions, memory and spatial perception). In addition, there were significant negative correlations between age of onset and atlas-based volumetry results for gray matter.

Conclusions: This study demonstrates a distinct pattern of DTI alterations of the white matter and ubiquitous volume reductions of the gray matter early in the disease course of *C9orf72*-associated ALS. Alterations were

Abbreviations: ABV, atlas-based volumetry; ALS, amyotrophic lateral sclerosis,; ALS-FRS-R, amyotrophic lateral sclerosis functional rating scale-revised; ASO, antisense oligonucleotide; BMI, body mass index; bvFTD, behavioral variant of frontotemporal dementia; CST, corticospinal tract; DTI, diffusion tensor imaging; ECAS, Edinburgh cognitive and behavioral amyotrophic lateral sclerosis screen; FA, fractional anisotropy; FDG PET, ^{8}F-2-fluoro-2-deoxy-D-glucose positron emission tomography; FDR, false-discovery rate; FTD, frontotemporal dementia; GM, gray matter; ICV, intracranial volume; LMN, lower motor neuron; MNI, Montreal neurological institute; MRI, magnetic resonance imaging; NfL, neurofilament light chain; p-NfH, phosphorylated neurofilament heavy chain; ROI, region of interest; RP-PCR, repeat-primed PCR; TDP-43, 43 kDa transactive response DNA-binding protein; UPN, upper motor neuron; WBSS, whole-brain based spatial statistics; WM, white matter.

* Corresponding author at: Department of Neurology, University Hospital Ulm, Oberer Eselsberg 45, D-89081 Ulm, Germany.
E-mail address: jan.kassubek@uni-ulm.de (J. Kassubek).

[1] Shared senior authorship.

https://doi.org/10.1016/j.nicl.2023.103505
Received 28 July 2023; Received in revised form 1 September 2023; Accepted 3 September 2023
Available online 9 September 2023

closely linked to a more aggressive cognitive phenotype. These results are in line with an expected pTDP43 propagation pattern of cortical affection and thus strengthen the hypothesis that an underlying developmental disorder is present in ALS with *C9orf72* expansions. Thus, multiparametric MRI could contribute to the assessment of the disease as an *in vivo* biomarker even in the early phase of the disease.

1. Introduction

Amyotrophic lateral sclerosis (ALS) is a progressive neurodegenerative disease, characterized by muscle weakness and a severely reduced life expectancy of about 2–5 years after diagnosis by irreversibly affecting the upper (UMN) and lower motor neurons (LMN) (Masrori and van Damme, 2020). In recent years, several disease-causing genes have been discovered (Brenner and Freischmidt, 2022), and among the genetic mutations, an expansion of the GGGGCC hexanucleotide in the non-coding region of *C9orf72* represents the most common cause of genetic ALS (DeJesus-Hernandez et al., 2011), with up to 41 % (Byrne et al., 2012; Müller et al., 2018) of familial and 5 % (Umoh et al., 2016) of seemingly sporadic cases. These expansions in *C9orf72* are also the most common genetic cause for the development of frontotemporal dementia (FTD) (DeJesus-Hernandez et al., 2011; Balendra and Isaacs, 2018; Renton et al., 2011) and cause FTD in 5–15 % of ALS patients (Wiesenfarth et al., 2023; Mandrioli et al., 2022). It could be shown that clinical features of ALS patients with *C9orf72* mutations differ from ALS patients without a causative gene mutation and from ALS patients carrying *SOD1* mutations (Wiesenfarth et al., 2023). A higher share of bulbar onset and female patients, faster disease progression rates in ALS-FRS-R, higher p-NfH levels in CSF, a larger percentage of neuropsychological deficits in ECAS and a shorter survival were reported for *C9orf72* mutation carriers (Wiesenfarth et al., 2023; Mandrioli et al., 2022; Gendron et al., 2017). None of these parameters were related to repeat lengths (Wiesenfarth et al., 2023).

Recently, it has been pointed out that there is a strong need to identify and establish sensitive biomarkers in ALS to simplify assessment of progression rate, to estimate prognosis, and to stratify patients in homogenous study groups. Such biomarkers may facilitate the evaluation of new therapeutic approaches (Feldman et al., 2022; Dreger et al., 2022), especially since anti-sense oligonucleotide (ASO)-based therapies are probed in ALS. Neurofilaments in CSF and plasma are described as promising in monitoring disease progression, severity and survival (Dreger et al., 2022; Benatar et al., 2020; Miller et al., 2022). Higher levels of NfL and p-NfH in blood and CSF were reported in ALS patients with *C9orf72* mutations as compared to ALS patients with *SOD1* mutations or without any known causative genetic mutation (Wiesenfarth et al. 2023; Benatar et al., 2020). Neuroimaging is another promising *in vivo* biomarker, particularly structural MRI to measure gray matter atrophy and diffusion tensor imaging (DTI) to assess alterations in structural white matter connectivity (Feldman et al., 2022; Floeter and Gendron, 2018). In ALS patients with *C9orf72* mutations, significant differences in structural MRI have been reported compared to ALS patients without these hexanucleotide expansions, especially in extramotor regions such as cortical and subcortical frontotemporal areas as well as the thalamus (Byrne et al., 2012; Floeter and Gendron, 2018; Bede et al., 2013; Agosta et al., 2017). Westeneng et al. reported widespread cortical alterations (Westeneng et al., 2016), and Agosta et al. described especially cerebellar and thalamic damage as well as occipital cortical thinning as findings in MRI of ALS patients with *C9orf72* mutations (Agosta et al., 2017). Nigri and colleagues recently reported cortical thinning in posterior brain regions extending to parietal, temporal and frontal areas in *C9orf72* ALS patients, also including subcortical gray matter (Nigri et al., 2023). Using DTI and tract-of-interest-based analysis, Müller and colleagues (Müller et al., 2020) demonstrated that *C9orf72*-positive ALS patients show a microstructural corticoefferent involvement according to the neuropathological staging pattern (Brettschneider et al., 2013) and, compared to controls, characteristically reduced FA values not only in callosal motor segment III but additionally in fibers of callosal segment II connecting to frontal regions (Müller et al., 2021).

In the current study, the assessment of structural MRI and DTI data in a multiparametric approach, comparison to $n = 51$ age-matched healthy controls as well as to $n = 51$ *C9orf72* negative ALS patients with a special focus on frontal involvement, and correlation analysis with clinical and neuropsychometric parameters in order to detect specific morphological patterns in MRI for potential *in vivo* biomarkers were performed for the first time in a large single-center cohort of $n = 51$ ALS patients with *C9orf72* mutations.

2. Material and methods

2.1. Subjects and patient characteristics

A total of $n = 51$ patients, who were diagnosed with definite, probable, or possible ALS according to revised El Escorial criteria (Ludolph et al., 2015) between 2012 and 2022 at the University of Ulm, Germany and who were positively tested for a GGGGCC hexanucleotide expansion in the *C9orf72* gene were enrolled in the study. Three ALS patients were additionally diagnosed with frontotemporal dementia of the behavioral type (bvFTD) according to Rascovsky criteria (Abrahams et al., 2015; Rascovsky et al., 2011). Data were compared to $n = 51$ age- and gender-matched healthy controls and $n = 51$ ALS patients who had been tested to be *C9orf72*-negative, respectively. All healthy control subjects had no family history of neuromuscular disease and had no history of neurologic, psychiatric, or other major medical illnesses and were recruited from among spouses of patients and by word of mouth. Gross brain pathology including vascular brain alterations was excluded by conventional MRI including fluid attenuation inversion recovery sequences. Age- and sex-match was tested by Kruskal-Wallis-test for the three groups and there were no significant differences ($p = 0.20$ for sex and $p = 0.15$ for age). Clinical features included site of onset, physical function according to the revised ALS functional rating scale (ALS-FRS-R) (Cedarbaum et al., 1999), progression rate (defined as average loss of ALS-FRS-R score per month), as well as average repeat lengths and phosphorylated neurofilament heavy chain (p-NfH) levels in CSF (Table 1). Although neurofilaments are markers for neuroaxonal damage and are found in different neurological diseases (ALS, Parkinson disease, multiple sclerosis, neurodegenerative dementia, stroke, traumatic brain injury) (Khalil et al., 2018), NfL/p-NfH were described to be significantly higher in MND (Steinacker et al., 2016), especially in *C9orf72* ALS (Gendron et al., 2017; Wiesenfarth et al., 2023), and therefore particularly suitable to discriminate between ALS and other neurodegenerative diseases (Gagliardi et al., 2021).

For cognitive testing, the German version of the Edinburgh Cognitive and Behavioral ALS Screen (ECAS) with age- and education-stratified cut-offs (Lulé et al., 2015; Loose et al., 2016) was performed in $n = 41$ *C9orf72* positive ALS patients (Table 2). Patients were screened for behavioral alterations using a peer evaluation by first degree relatives (partners or children). For this, the behavioral scale of the ECAS was used, based on the guidelines for diagnosing behavioral variant FTD according to the Rascovsky criteria (Abrahams et al., 2014). Of the 28 patients with available reports, $n = 10$ provided evidence for behavioral alteration in one behavioral domain (all apathy), and $n = 6$ subjects presented with alterations in two or more behavioral domains (up to five), of whom $n = 3$ fulfilled the criteria of full-blown ALS-bvFTD. There was no evidence for the presence of psychotic symptoms.

Table 1
Subject characteristics. ALS-FRS-R: ALS Functional Rating Scale-Revised, ECAS: Edinburgh Cognitive and Behavioral ALS Screen, p-NfH: phosphorylated neurofilament heavy chain. P-values were calculated with Kruskal-Wallis-test for the three group comparisons. For two group comparisons between *C9orf72* positive and *C9orf72* negative ALS patients unpaired Student's *t*-test was used for continuous variables, Mann-Whitney-*U* test for ordinal variables and Chi-Square-test for nominal variables.

	***C9orf72* positive ALS patients ($n = 51$)**	***C9orf72* negative ALS patients ($n = 51$)**	**healthy controls ($n = 51$)**	**p-values**
Age (mean, SD)	61.1 ± 9.1	64.1 ± 10.7	61.4 ± 7.4	0.15
Age of onset (median, IQR)	58.0 (53.0–66.0)	63.0 (56.8–69.3)		0.13
Sex				
male	54.9 % ($n = 28$)	64.7 % ($n = 33$)	45.1 % ($n = 23$)	
female	45.1 % ($n = 23$)	35.3 % ($n = 18$)	54.9 % ($n = 28$)	0.20
Onset				
spinal	70.8 % ($n = 34$)	75.0 % ($n = 12$)		
bulbar	29.2 % ($n = 14$)	25.0 % ($n = 4$)	0.75	
Type				
sporadic	54.9 % ($n = 28$)	100 % ($n = 51$)		
familial	45.1 % ($n = 23$)			
Handedness				
right	96.0 % ($n = 49$)	92.1 % ($n = 47$)		
left	4.0 % ($n = 2$)	7.4 % ($n = 4$)	0.90	
ALS-FRS-R (1st visit) (median, IQR)	40.0 (38.5–43.0) ($n = 51$)	42.0 (35.0–45.0) ($n = 50$)		0.86
Progression Rate (median, IQR) (1st to last visit)	−1.1 (-0.6–1.5) ($n = 23$)	−0.55 (-0.20–1.29) ($n = 27$)		0.14
Diagnostic delay in months (median, IQR)	8.0 (5.0–16.0) ($n = 51$)	9.5 (4.0–15.5) ($n = 50$)		0.66
Survival in months (median, IQR)	29.5 (23.3–33.0) ($n = 16$)	21.0 (16.0–34.0) ($n = 27$)		0.42
p-NfH (pg/ml)	2487 (1283–3678) ($n = 30$)			
ECAS total score (median, IQR)	100.0 (86.0–110.0) ($n = 41$)	103.5 (89.0–110.3) ($n = 26$)		0.48

Table 2
Neuropsychological characteristics in the Edinburgh Cognitive and Behavioral Screen (ECAS). ALS: Amyotrophic lateral sclerosis, ECAS: Edinburgh Cognitive and Behavioral ALS Screen.

	maximum	***C9orf72* ($n = 41$)**
Non ALS specific score (median, IQR)	36	25.0 (22.0–29.0)
Memory (median, IQR)	24	14.0 (11.5–17.0)
Spatial perception (median, IQR)	12	12.0 (11.0–12.0)
ALS specific score (median, IQR)	100	76.0 (64.5–80.5)
Verbal fluency (median, IQR)	24	16.0 (12.0–18.0)
Language (median, IQR)	28	24.0 (20.5–26.5)
Executive functions (median, IQR)	48	34.0 (32.0–38.0)
Total score (median, IQR)	136	100.0 (86.0–110.0)

All subjects included in the study received MRI during routine clinical diagnostic procedures at the Department of Neurology, University of Ulm, Germany between 2010 and 2022. Gross brain pathology, including relevant vascular brain alterations, were excluded by conventional MRI with fluid-attenuated inversion recovery sequences. The MRI scans of *C9orf72* positive ALS patients were performed early in the course of the disease, i.e., 11.0 months after onset of disease (median; IQR, 6.0–18.0 months) and 8.5 days after diagnosis (median; IQR −5.0–120.5 days). In the *C9orf72* negative ALS patients, MRI was performed 9.5 months after onset of disease (median; IQR, 6.8–18.5 months) and 4.0 days after diagnosis (median; IQR −6.3–84.8 days).

All subjects provided written informed consent. The study was approved by the institutional Ethics Committee of the University of Ulm (reference # 19/12) and has therefore been performed in accordance with the ethical standards laid down in the 1964 Declaration of Helsinki and its later amendments.

2.2. Genetic analysis

DNA was extracted from blood leucocytes. Analysis of the *C9orf72* repeat length was performed by fragment length analysis and repeat-primed PCR (RP-PCR) (DeJesus-Hernandez et al., 2011; Renton et al., 2011). Electrophoresis was performed on an ABI PRISM® 3130 Genetic Analyzer (Life Technologies, Foster City, California, USA). The data were analyzed using the Peak Scanner software (Applied Biosystems, Waltham, Massachusetts, USA). Samples with a saw tooth pattern in the RP-PCR were further analyzed using Southern blot (Hübers et al., 2014). Genetic testing was performed at the Institute of Human Genetics of Ulm University.

2.3. Magnetic resonance imaging acquisition

Magnetic resonance imaging (MRI) scans were obtained on a 1.5 Tesla Magnetom Symphony scanner (Siemens Medical, Erlangen, Germany); the T1-weighted imaging (Magnetization Prepared Rapid Acquisition with Gradient Echo, MPRAGE) consisted of 144 sagittal slices of 1.2 mm thickness, 1.0 mm × 1.0 mm in-plane resolution in a 256 × 248 matrix, echo time (TE) was 4.2 ms, repetition time (TR) was 1640 ms. The diffusion tensor imaging (DTI) study protocol consisted of 52 volumes (64 slices, 128x128 pixels, slice thickness 2.8 mm, in-plane pixel size 2.0 mm × 2.0 mm), representing 48 gradient directions (b = 1000 s/mm^2) and four scans with b = 0, TE and TR were 95 ms and 8000 ms.

2.4. Structural MRI analysis – Atlas-based volumetry

The T1-weighted data were processed by use of MATLAB (version R2014b, The Mathworks, USA) using the Statistical Parametric Mapping 12 (SPM12) software (Wellcome Trust Center for Neuroimaging, London, UK, www. fil.ion.ucl.ac.uk/spm) according to a standardized processing pipeline for ABV (Huppertz et al., 2016). Briefly, processing included (i) segmentation into gray matter (GM), white matter (WM) and cerebro-spinal fluid (CSF) compartments, (ii) stereotaxic normalization into Montreal Neurological Institute (MNI) space, (iii) and volumetric assessment using voxel-by-voxel multiplication and subsequent integration of normalized modulated component images (GM, WM or CSF) with predefined masks from different brain atlases. To enhance the quality of mapping into atlas space, high-dimensional registration methods have been introduced, and the intrascanner variability of volumetric results was shown to be < 1% for the majority of investigated structures (Opfer et al., 2016). The technique of ABV has been successfully employed in cross-sectional and longitudinal studies (Kassubek et al., 2011; Frings et al., 2012; Höglinger et al., 2014; Huppertz et al., 2016). All volumetric results have been linearly standardized to the mean intracranial volume (ICV) of controls. Differences at the group level were tested for significance after correction for multiple comparisons. Correlation analysis (Spearman rank correlation) with clinical parameters was performed for volumetric results of all analyzed regions.

2.5. Microstructural MRI analysis – Diffusion tensor imaging (DTI)

The DTI analysis software *Tensor Imaging and Fibre Tracking* (Müller et al., 2007) was used for postprocessing and statistical analysis; the algorithms have been previously described in detail (Kassubek et al., 2018; Kalra et al., 2020). In brief, after correction for eddy-currents and a standardized quality control protocol, stereotaxic normalization to the

Montreal Neurological Institute (MNI) space was performed iteratively using study-specific templates. To map white matter microstructure, from the stereotaxically normalized DTI, data sets of all subjects' fractional anisotropy (FA) maps were calculated. A Gaussian filter of 8 mm full width at half maximum was applied for smoothing of FA maps for a good balance between sensitivity and specificity. Finally, FA maps were corrected for the covariate age. Statistical comparison by Mann-Whitney-test was performed voxel-wise for FA values to detect changes between the subject groups (whole brain-based spatial statistics, WBSS). Voxels with FA values below 0.2 were not considered for statistical comparison, since cortical grey matter shows FA values up to 0.2. Statistical results were corrected for multiple comparisons using the false-discovery rate (FDR) algorithm at $p < 0.05$. Further reduction of the alpha error was performed by a spatial correlation algorithm leading to a threshold cluster size of 512 voxels (for further information, cf. (Kassubek et al., 2018; Kalra et al., 2020). For the correlation analyses, spherical regions of interest (ROIs) were automatically placed bihemispherically within the peak results clusters of WBSS, i.e., in the upper CST (MNI ± 22/-25/38, diameter 20 mm), lower CST (MNI ± 18/-25/0, diameter 20 mm), and frontal lobes (MNI ± 22/35/1, diameter 20 mm); FA values within these ROIs were arithmetically averaged (Fig. 1).

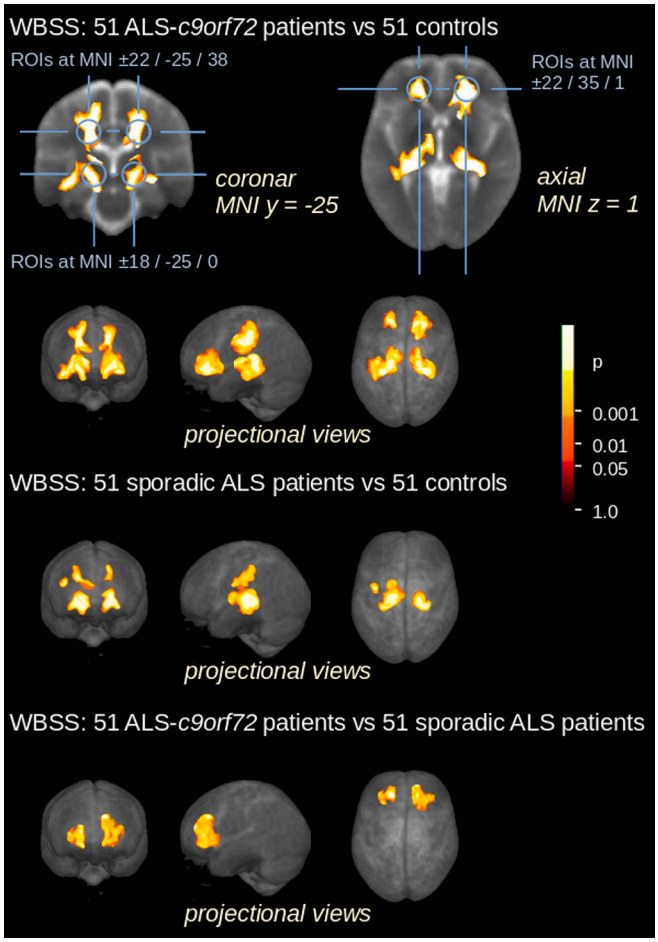

Fig. 1. White matter integrity analysis with whole brain-based spatial statistics (WBSS) of 51 ALS patients carrying *C9orf72* mutations versus 51 controls and versus 51 *C9orf72* negative ALS patients. (upper panel) 51 ALS patients carrying *C9orf72* mutations versus 51 controls in slicewise view showing localizations of ROIs for correlation analysis as well as projectional views. ROIs were located at bilateral alterations in the corticospinal tracts (CST) (MNI ± 22/-25/38 and ± 18/-25/0) and at bilateral alterations in the frontal lobes (MNI ± 22/35/1). **(central panel)** projectional pseudo 3D views of alterations of 51 *C9orf72* negative ALS patients versus 51 controls. **(lower panel)** projectional pseudo 3D views of alterations of 51 ALS patients carrying *C9orf72* mutations versus 51 *C9orf72* negative ALS patients. MNI: Montreal Neurological Institute.

2.6. Association between clinical features and ROI analysis

Correlation analysis (Spearman rank correlation) with clinical parameters was performed for averaged FA values from all ROIs in the *C9orf72* positive ALS patients.

3. Results

3.1. Microstructural alterations

At group level, the WBSS-based comparison of both ALS groups (n = 51 ALS patients carrying *C9orf72* mutations versus *C9orf72* negative ALS patients, respectively) with the n = 51 age-matched controls showed significant bilateral alterations in white matter axonal structures at FDR-corrected $p < 0.05$ projecting bilaterally to the upper and lower CSTs. Additionally, the group of the ALS patients carrying *C9orf72* mutations showed alterations in the frontal lobes when compared to controls. This involvement of the frontal lobes in the group of the ALS patients carrying *C9orf72* mutations was also detected when compared to the group of *C9orf72* negative ALS patients (Fig. 1). The localizations of clusters with decreased FA were consecutively used as ROIs for correlation analyses (see sections 3.3. and 3.4.). Details of WBSS cluster results are summarized in Table 3.

3.2. Structural alterations

In the ABV analysis, as summarized in Table 4, ALS patients with *C9orf72* mutations had lower volumes of the whole brain, including frontal, temporal and parietal lobes ($p < 0.001$) compared to healthy controls. These differences were based especially on lower values of the

Table 3
WBSS of FA maps – 51 ALS-*c9orf72* patients vs 51 controls, 51 *C9orf72* negative ALS patients vs 51 controls, and 51 ALS-*c9orf72* patients vs 51 *C9orf72* negative ALS patients. ALS: Amyotrophic lateral sclerosis, MNI: Montreal Neurological Institute, CST: corticospinal tract.

cl. no.	no. of voxels	MNI (x/y/z)	p	anatomical localization
ALS-*c9orf72* patients vs controls				
1	14,548	−17 / −24 / 4	< 0.000001	lower CST L
2	11,756	22 / 36 / 3	< 0.000001	frontal lobe R
3	11,510	−20 / −27 / 39	< 0.000001	upper CST L
4	8851	22 / −26 / 40	< 0.000001	upper CST R
5	8522	20 / −27 / 6	< 0.000001	lower CST R
6	5199	−20 / 33 / 0	< 0.000001	frontal lobe L
***C9orf72* negative ALS patients vs controls**				
7	12,126	−17 / −26 / −1	< 0.000001	lower CST L
8	8253	16 / −27 / −3	< 0.000001	lower CST R
9	6054	−17 / −21 / 29	< 0.000001	upper CST L
10	2415	21 / −26 / 40	< 0.000001	upper CST R
11	1183	−43—6 24	< 0.000001	temporal lobe
ALS-*c9orf72* patients vs *C9orf72* negative ALS patients				
12	14,095	22 / 36 / 3	< 0.000001	frontal lobe R
13	7397	−20 / 33 / 0	< 0.000001	frontal lobe L

Table 4

Results of volumetric MRI analysis. Volume results are shown in mm^3, results for planes in mm^2. All results have been standardized to the mean intracranial volume (ICV) of controls. A three-color scale was used to rank the percentage volume difference of ALS patients with *C9orf72* mutations to healthy controls and *C9orf72* negative ALS, from shades of red (volume loss) over white (control level) to shades of blue (volume gain). All p-values were adjusted with Bonferroni-Holm equation for multiple testing. GM: Gray Matter, ns: not statistically significant, WM: White Matter, SD: standard deviation.

	Patients		**Healthy controls**		**z scores**	**p-values**
	Mean	**SD**	**Mean**	**SD**		
Brain	994,6	67,1	1067,6	40,4	−1,8	<0.001
Gray Matter	516,8	52,7	600,9	35,6	−2,4	<0.001
White Matter	477,8	33,4	466,7	26,4	0,4	ns
CSF	405,4	67,1	332,4	40,4	1,8	<0.001
Cerebrum	848,6	59,2	915,0	37,5	−1,8	<0.001
Cerebrum GM	424,3	45,7	499,4	30,8	−2,4	<0.001
Cerebrum WM	424,3	30,6	415,6	25,9	0,3	ns
Cerebral cortex	408,8	43,9	480,9	29,8	−2,4	<0.001
Cerebral subcortex	357,1	26,6	348,3	22,6	0,4	ns
Frontal lobe	277,3	21,7	305,1	17,1	−1,6	<0.001
Frontal lobe GM	138,4	15,5	165,8	11,4	−2,4	<0.001
Frontal lobe WM	138,9	10,8	139,3	10,4	0,0	ns
Temporal lobe	171,0	13,8	184,5	8,5	−1,6	<0.001
Temporal lobe GM	109,5	12,3	125,2	7,5	−2,1	<0.001
Temporal lobe WM	61,5	4,7	59,3	4,1	0,6	ns
Parietal lobe	156,3	11,1	168,7	9,0	−1,4	<0.001
Parietal lobe GM	76,4	9,2	91,0	7,6	−1,9	<0.001
Parietal lobe WM	79,9	6,8	77,7	5,6	0,4	ns
Occipital lobe	112,3	8,8	118,3	6,7	−0,9	0.004
Occipital lobe GM	55,2	6,5	65,6	5,7	−1,8	<0.001
Occipital lobe WM	57,1	5,9	52,7	4,4	1,0	<0.001
Insula	14,2	1,6	15,8	1,1	−1,5	<0.001
Striatum	13,9	2,0	15,4	1,4	−1,1	<0.001
Hippocampus	5,1	0,8	6,1	0,5	−2,1	<0.001
Amygdala	2,9	0,4	3,3	0,3	−1,6	<0.001
Caudate	3,1	0,7	3,8	0,4	−1,6	<0.001
Putamen	5,1	0,7	5,4	0,6	−0,5	ns
Accumbens	0,8	0,1	0,9	0,1	−1,1	<0.001
Pallidum	3,6	0,3	3,8	0,2	−0,8	0.005
Thalamus	9,7	1,2	11,4	0,7	−2,4	<0.001
Cerebellum	108,1	9,5	113,7	8,3	−0,7	0.04
Cerebellum GM	82,0	8,8	89,8	7,2	−1,1	<0.001
Cerebellum WM	26,1	2,3	23,9	2,1	1,1	<0.001
Brainstem	30,0	2,3	30,2	1,7	−0,1	ns
Midbrain	10,1	0,7	10,2	0,5	−0,2	ns
Pons	15,5	1,5	15,5	1,1	0,0	ns
Medulla	4,4	0,4	4,6	0,3	−0,4	ns
Corpus callosum plane	620,7	77,8	615,5	78,1	0,1	ns
Cerebellar vermis plane	956,7	85,4	979,6	68,4	−0,3	ns
Midbrain plane	269,1	30,2	286,9	20,9	−0,9	0.02
Midbrain tegmentum plane	163,9	16,9	167,7	11,6	−0,3	ns
Pons plane	511,1	47,8	507,5	38,1	0,1	ns
Pons pars basilaris plane	349,4	33,1	347,7	26,3	0,1	ns
Medulla plane	256,1	23,8	260,7	19,4	−0,2	ns
	Patients		***C9orf72* negative ALS**		**z scores**	**p-values**
	Mean	**SD**	**Mean**	**SD**		
Brain	994,6	67,1	1020,0	57,7	−0,4	ns
Gray Matter	516,8	52,7	550,5	45,6	−0,7	ns
White Matter	477,8	33,4	469,4	36,2	0,2	ns
CSF	405,4	67,1	380,0	57,7	0,4	ns
Cerebrum	848,6	59,2	874,1	53,8	−0,5	ns
Cerebrum GM	424,3	45,7	455,6	42,0	−0,7	0.04
Cerebrum WM	424,3	30,6	418,5	33,8	0,2	ns
Cerebral cortex	408,8	43,9	438,5	40,9	−0,7	0.04
Cerebral subcortex	357,1	26,6	351,2	29,4	0,2	ns
Frontal lobe	277,3	21,7	289,2	21,8	−0,5	ns
Frontal lobe GM	138,4	15,5	151,1	16,2	−0,8	0.01
Frontal lobe WM	138,9	10,8	138,1	13,4	0,1	ns
Temporal lobe	171,0	13,8	174,3	13,1	−0,3	ns
Temporal lobe GM	109,5	12,3	114,1	10,8	−0,4	ns
Temporal lobe WM	61,5	4,7	60,2	5,3	0,3	ns
Parietal lobe	156,3	11,1	161,3	10,0	−0,5	ns
Parietal lobe GM	76,4	9,2	83,1	7,9	−0,9	0.01
Parietal lobe WM	79,9	6,8	78,1	7,6	0,2	ns
Occipital lobe	112,3	8,8	115,0	8,5	−0,3	ns
Occipital lobe GM	55,2	6,5	59,7	6,9	−0,7	ns
Occipital lobe WM	57,1	5,9	55,3	4,9	0,4	ns
Insula	14,2	1,6	14,8	1,5	−0,4	ns
Striatum	13,9	2,0	14,5	1,6	−0,4	ns

(*continued on next page*)

Table 4 (*continued*)

	Patients		*C9orf72* negative ALS		z scores	p-values
	Mean	SD	Mean	SD		
Hippocampus	5,1	0,8	5,3	0,7	−0,2	ns
Amygdala	2,9	0,4	2,9	0,4	−0,1	ns
Caudate	3,1	0,7	3,4	0,6	−0,4	ns
Putamen	5,1	0,7	5,2	0,6	−0,2	ns
Accumbens	0,8	0,1	0,9	0,1	−0,4	ns
Pallidum	3,6	0,3	3,6	0,2	−0,2	ns
Thalamus	9,7	1,2	10,6	1,0	−0,9	0.004
Cerebellum	108,1	9,5	108,9	9,0	−0,1	ns
Cerebellum GM	82,0	8,8	84,0	7,8	−0,3	ns
Cerebellum WM	26,1	2,3	24,9	2,4	0,5	ns
Brainstem	30,0	2,3	29,0	2,0	0,5	ns
Midbrain	10,1	0,7	10,0	0,6	0,2	ns
Pons	15,5	1,5	14,8	1,3	0,5	ns
Medulla	4,4	0,4	4,3	0,4	0,3	ns
Corpus callosum plane	620,7	77,8	608,8	79,0	0,2	ns
Cerebellar vermis plane	956,7	85,4	969,6	84,8	−0,2	ns
Midbrain plane	269,1	30,2	277,3	29,1	−0,3	ns
Midbrain tegmentum plane	163,9	16,9	168,2	16,2	−0,3	ns
Pons plane	511,1	47,8	494,1	44,7	0,4	ns
Pons pars basilaris plane	349,4	33,1	335,1	30,2	0,5	ns
Medulla plane	256,1	23,8	247,2	24,9	0,4	ns

gray matter in these regions. Also compared with the *C9orf72* negative ALS patients, the differences were statistically significant for gray matter of the whole cerebrum ($p = 0.04$) as well as in frontal ($p = 0.01$) and parietal lobes ($p = 0.01$). The total volumes of the occipital lobe ($p = 0.004$) and the cerebellum ($p = 0.04$) were also lower in *C9orf72* patients compared to healthy controls and on gyral level (GM of left

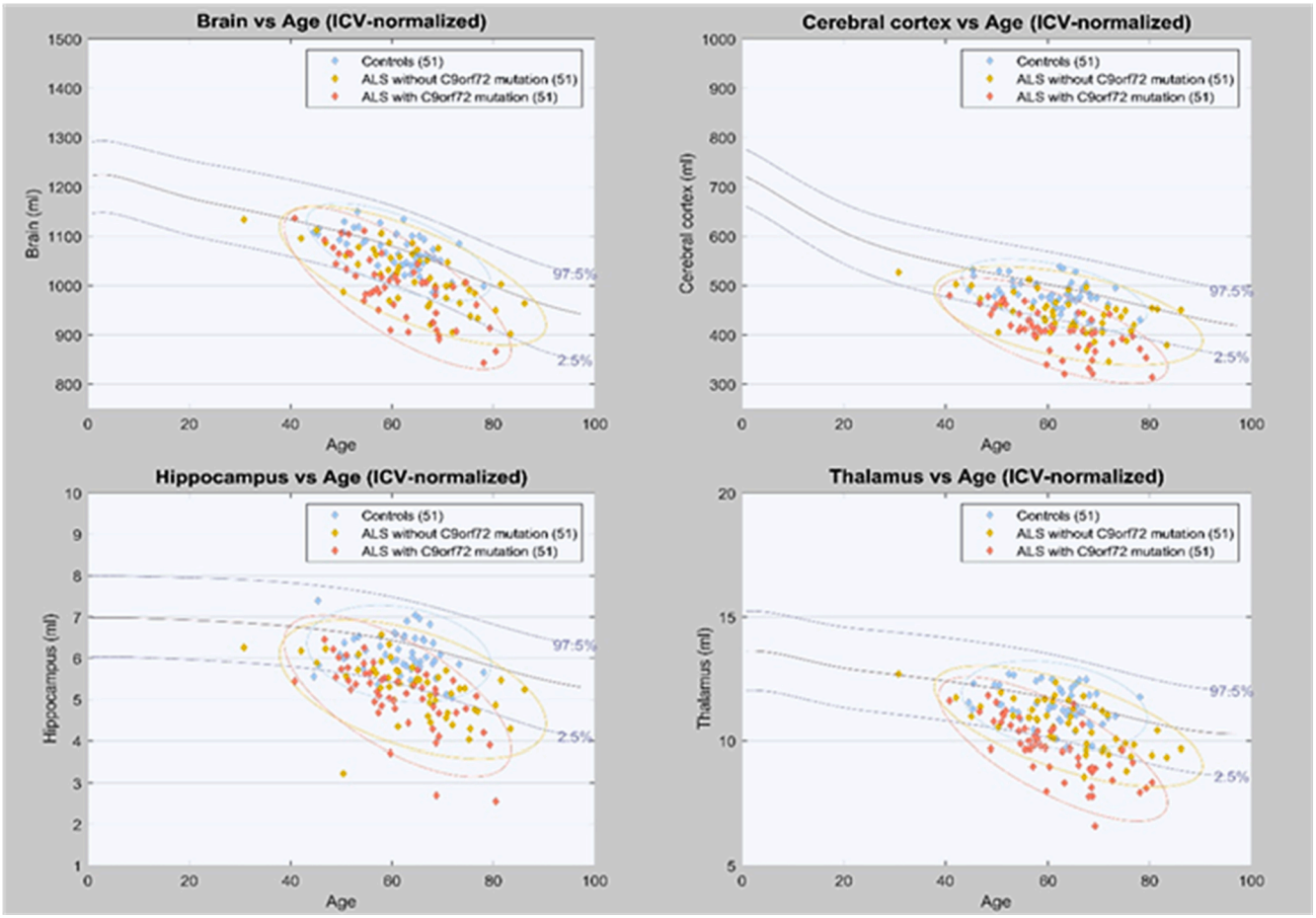

Fig. 2. Analysis of brain volumes over age, normalized to the mean intracranial volume (ICV) (A) Whole brain **(B)** Cerebral cortex **(C)** Hippocampus **(D)** Thalamus. GM: gray matter. Scatter plots with volumes of the respective brain regions (A-D) in ml on the y-axis vs. age in years on the x-axis. Red: *C9orf72*-associated ALS patients. Blue: Healthy controls. Yellow: ALS patients without *C9orf72* mutations. Dashed lines: 2.5 and 97.5 percentiles of a larger control group (not part of this study, courtesy of Prof. Hans-Jürgen Huppertz, Zürich, Switzerland). (For interpretation of the references to color in this figure legend, the reader is referred to the web version of this article.)

superior occipital gyrus and bilateral middle occipital gyri) to *C9orf72* negative ALS patients. In addition, volumes of hippocampi and amygdala ($p < 0.001$) were lower in *C9orf72* ALS patients, however, these differences were statistically significant only in the comparison to healthy controls. Beyond the whole cerebral gray matter values, the most pronounced differences between *C9orf72* ALS patients and healthy controls ($p < 0.001$) and *C9orf72* negative ALS patients ($p = 0.004$), respectively, were observed in the thalamus. Compared to healthy controls, lower values were also obtained in the basal ganglia (striatum) ($p < 0.001$), whereas no differences to controls could be observed in brainstem, midbrain, pons and medulla oblongata. In line with the results of decreased whole brain volume, the volume of the CSF spaces was increased *e vacuo* in ALS patients with *C9orf72* mutations compared to the matched healthy controls ($p < 0.001$). Examples of reduced volumes are shown in Fig. 2 for whole brain, cerebrum, cerebral cortex and hippocampus in *C9orf72* ALS.

Differences in gray matter volumes between *C9orf72* ALS patients and controls were also analyzed at gyral level (Table 5), and gray matter volumes were lower in all gyri bilaterally in *C9orf72* patients. The lowest values compared to healthy controls were measured in the superior frontal and in the precentral gyrus, whereas the lowest differences in gray matter were observed in the inferior occipital cortex. In addition to decreased volumes in the precentral gyrus ($p = 0.03$), lower volumes were also obtained in the frontal lobe (left superior frontal gyrus ($p = 0.02$), left middle frontal gyrus ($p = 0.01$), right middle frontal gyrus ($p = 0.04$), right inferior frontal gyrus ($p = 0.02$)), angular gyri ($p = 0.03$ and $p < 0.001$, respectively), and middle occipital gyri ($p < 0.05$ and $p < 0.001$, respectively), compared to *C9orf72* negative ALS patients. Of note, no significant differences in gray and white matter volumes between right and left hemisphere were observed in this study.

3.3. Correlation between neuropsychological results in ECAS and ROI analysis

The correlation analysis between ECAS and ROI-based FA values of frontal association fibers, upper and lower CST revealed significant correlations between cognitive performance and frontal association fibers. Lower FA values in the frontal lobes were associated with worse performance in language ($r = 0.40$, $p = 0.03$), verbal fluency ($r = 0.34$, $p = 0.04$), executive functions ($r = 0.45$, $p = 0.02$), memory ($r = 0.36$, $p = 0.04$), spatial perception ($r = 0.52$, $p = 0.003$), ALS specific ($r = 0.53$, $p = 0.003$), non ALS specific ($r = 0.42$, $p = 0.03$) and ECAS total score ($r = 0.50$, $p = 0.001$), respectively (Table 6). No statistically significant correlations were found between neuropsychological results in ECAS and ROI-based FA values of lower and upper CST. Furthermore, there were no statistically significant correlations between behavioral alterations, detected in the behavioral scale of the ECAS, and FA values in DTI.

3.4. Correlation between clinical features and ROI analysis

A significant correlation between age of onset and FA values in frontal lobes, but not the corticospinal tracts was observed. A higher age of onset was correlated with lower FA values ($r = -0.40$, $p = 0.03$).

3.5. Correlation between neuropsychological results in ECAS and atlas-based volumetry

Significant correlations were obtained between neuropsychological results in ECAS total score and ABV results for whole brain ($r = 0.43$, $p = 0.04$), whole cerebrum ($r = 0.44$, $p = 0.03$), gray matter of middle frontal cortex ($r = 0.42$, $p < 0.05$ right and $r = 0.47$, $p = 0.01$ left), gray matter of right superior parietal cortex ($r = 0.46$, $p = 0.01$), and left supramarginal gyrus ($r = 0.45$, $p = 0.04$), but also for basal ganglia (striatum, caudate, ncl. accumbens) and regions of the midbrain. Interestingly, volumetric results of midbrain (midbrain plane, tegmentum midbrain plane) and basal ganglia were also strongly correlated with ECAS subdomains (Supplementary Table S1). After adjusting for multiple comparisons, correlation analysis between ABV results and behavioral data in ECAS did not show any significant results.

3.6. Correlation between clinical features and atlas-based volumetry

A correlation of clinical features (onset, family history, ALS-FRS-R, progression rate as ALS-FRS-R loss/month, survival, p-NfH in CSF, ECAS total score and subdomains) and ABV data with Spearman coefficient showed no significant results after adjusting p-values for multiple testing with Bonferroni-Holm. A single negative correlation was found between white matter in the temporal lobes ($r = -0.54$; $p = 0.006$) and GGGGCC hexanucleotide repeat length. Negative correlations were observed between age of onset and the volume of whole brain, basal ganglia, midbrain, medulla and cerebellum (Supplementary Table S2). Significant negative correlations also existed between age of onset and gray matter.

4. Discussion

In this neuroimaging-based combined gray and white matter analysis, we demonstrated global volume reductions of the gray matter and reduced FA values in white matter structures of the corticospinal tract and fibers projecting to the frontal lobes in ALS patients with *C9orf72* mutations. Significant correlations between alterations in MRI and clinical features were observed between FA values in frontal association fibers and cognitive performance; furthermore, neuropsychological results in ECAS showed significant correlations with ABV for whole brain, cerebrum, and single gyri of the frontal and parietal cortex, but also for basal ganglia and the midbrain.

Of note, the gray matter volumes in ALS patients with *C9orf72* mutations compared to controls were lower in our study across several brain regions. These areas are known to be consecutively affected by soluble phosphorylated 43 kDa transactive response DNA-binding protein (TDP-43) aggregation as the underlying pathology of sporadic and many familial forms of ALS and FTD (Brettschneider et al., 2015; Lee et al., 2011). According to the pivotal neuropathological studies (Braak et al., 2013; Brettschneider et al., 2013), TDP-43 pathology in ALS can be detected first in the motor cortex (stage 1) and sequentially in other brain regions like the prefrontal neocortex and brainstem (stage 2), the orbitofrontal areas, the postcentral neocortex and the striatum (stage 3) and finally, the temporal lobes including the hippocampi (stage 4). The core findings of the current study are in accordance with this pattern for which no differences in the distribution pattern, but a greater burden of TDP43 pathology was reported for ALS patients with *C9orf72* mutations in the original publication ($n = 11$; Brettschneider et al., 2013). Thus, the current findings are in line with the concept of ALS to be primarily a disease of the cerebral neocortex projecting secondarily to other CNS regions along corticofugal axons (Braak et al., 2013).

The volume reductions in our study were most prominent in the gray matter of the superior frontal and the precentral gyrus. However, as we could also observe reduced volumes of structures like the hippocampi which are considered to be affected later in the disease course (Braak et al., 2013), these findings may either indicate that some subjects presented with advanced cerebral TDP43 pathology which is only to a limited extent associated with clinical presentation according to ALS-FRS-R (Braak et al., 2013). On the other hand, these results may as well imply that the observed ubiquitous volume reduction of gray matter corresponds to general neurodevelopmental disruptions (Lulé et al., 2020). It has been already described that *C9orf72* is important for the development of the central nervous system (Yeh et al., 2018). Alterations in frontal and parietal cortices as well as in connecting fibers to frontal regions were already present in presymptomatic *C9orf72* gene carriers (Bertrand et al., 2018), and a reduction in gray and white matter was reported to be present already in early adulthood with no further

Table 5

Results of volumetric MRI analysis at gyral level. Volume results are shown in mL, results for planes in mm^2. All results have been standardized to the mean intracranial volume (ICV) of controls. A three-color scale was used to rank the percentage volume difference of ALS patients with *C9orf72* mutations to healthy controls and *C9orf72* negative ALS, from shades of red (volume loss) over white (control level) to shades of blue (volume gain). All p-values were adjusted with Bonferroni-Holm equation for multiple testing. GM: Gray Matter, L: left, ns: not statistically significant, R: right, SD: standard deviation.

	Gray matter Patients		**Healthy controls**		**z scores**	**p-values**
	Mean	**SD**	**Mean**	**SD**		
Superior frontal gyrus R	23,6	2,6	27,9	2,0	−2,2	<0.001
Superior frontal gyrus L	23,6	2,5	28,0	2,0	−2,2	<0.001
Middle frontal gyrus R	18,8	2,4	22,2	2,0	−1,8	<0.001
Middle frontal gyrus L	18,7	2,4	22,1	1,8	−1,9	<0.001
Inferior frontal gyrus R	10,3	1,5	12,7	1,2	−2,0	<0.001
Inferior frontal gyrus L	9,7	1,5	11,8	1,1	−1,9	<0.001
Precentral gyrus R	7,9	1,1	10,0	0,9	−2,3	<0.001
Precentral gyrus L	8,6	1,0	10,6	0,9	−2,2	<0.001
Middle orbitofrontal gyrus R	4,8	0,5	5,6	0,4	−2,0	<0.001
Middle orbitofrontal gyrus L	4,6	0,6	5,4	0,5	−1,6	<0.001
Lateral orbitofrontal gyrus R	2,4	0,4	2,9	0,3	−1,8	<0.001
Lateral orbitofrontal gyrus L	2,5	0,4	3,1	0,3	−1,8	<0.001
Gyrus rectus R	1,5	0,2	1,8	0,2	−1,7	<0.001
Gyrus rectus L	1,5	0,2	1,7	0,1	−1,6	<0.001
Postcentral gyrus R	6,4	0,9	7,5	0,8	−1,5	<0.001
Postcentral gyrus L	7,1	1,1	8,4	0,9	−1,5	<0.001
Superior parietal gyrus R	10,0	1,4	12,0	1,4	−1,4	<0.001
Superior parietal gyrus L	10,2	1,3	12,1	1,3	−1,5	<0.001
Supramarginal gyrus R	6,5	1,1	7,7	0,9	−1,4	<0.001
Supramarginal gyrus L	7,1	1,1	8,6	0,9	−1,6	<0.001
Angular gyrus R	9,3	1,1	11,0	0,9	−1,8	<0.001
Angular gyrus L	8,6	1,2	10,3	1,1	−1,6	<0.001
Precuneus R	5,6	0,6	6,7	0,7	−1,5	<0.001
Precuneus L	5,6	0,6	6,7	0,9	−1,3	<0.001
Superior occipital gyrus R	3,0	0,5	3,9	0,4	−2,0	<0.001
Superior occipital gyrus L	2,7	0,5	3,6	0,5	−1,9	<0.001
Middle occipital gyrus R	9,2	1,2	10,8	1,0	−1,5	<0.001
Middle occipital gyrus L	8,6	1,1	10,4	1,3	−1,3	<0.001
Inferior occipital gyrus R	5,3	0,7	5,8	0,5	−0,9	0.004
Inferior occipital gyrus L	5,4	0,7	6,0	0,6	−1,0	<0.001
Cuneus R	3,1	0,5	3,7	0,4	−1,4	<0.001
Cuneus L	2,2	0,5	2,9	0,5	−1,4	<0.001
Superior temporal gyrus R	14,0	2,1	16,5	1,4	−1,8	<0.001
Superior temporal gyrus L	15,9	2,3	18,3	1,5	−1,6	<0.001
Middle temporal gyrus R	12,7	1,4	14,7	1,1	−1,8	<0.001
Middle temporal gyrus L	12,6	1,4	14,4	1,1	−1,6	<0.001
Inferior temporal gyrus R	11,4	1,1	12,6	0,8	−1,5	<0.001
Inferior temporal gyrus L	11,1	1,3	12,4	0,9	−1,5	<0.001
Parahippocampal gyrus R	4,2	0,5	4,7	0,4	−1,3	<0.001
Parahippocampal gyrus L	3,8	0,5	4,3	0,3	−1,7	<0.001
Lingual gyrus R	8,1	1,1	9,5	0,9	−1,6	<0.001
Lingual gyrus L	7,5	1,0	9,0	0,9	−1,7	<0.001
Fusiform gyrus R	7,3	0,8	8,2	0,6	−1,6	<0.001
Fusiform gyrus L	7,6	0,8	8,5	0,6	−1,5	<0.001
Cingulate gyrus R	7,5	0,8	8,7	0,8	−1,6	<0.001
Cingulate gyrus L	7,6	0,9	8,8	0,8	−1,6	<0.001
	Gray matter Patients		***C9orf72* negative ALS**		**z scores**	**p-values**
	Mean	**SD**	**Mean**	**SD**		
Superior frontal gyrus R	23,6	2,6	25,5	3,0	−0,6	ns
Superior frontal gyrus L	23,6	2,5	25,6	2,7	−0,7	0.02
Middle frontal gyrus R	18,8	2,4	20,5	2,6	−0,7	0.04
Middle frontal gyrus L	18,7	2,4	20,6	2,5	−0,8	0.01
Inferior frontal gyrus R	10,3	1,5	11,4	1,4	−0,8	0.02
Inferior frontal gyrus L	9,7	1,5	10,6	1,2	−0,8	ns
Precentral gyrus R	7,9	1,1	8,7	1,1	−0,7	0.03
Precentral gyrus L	8,6	1,0	9,5	1,5	−0,6	0.03
Middle orbitofrontal gyrus R	4,8	0,5	5,2	0,6	−0,6	ns
Middle orbitofrontal gyrus L	4,6	0,6	5,0	0,5	−0,7	ns
Lateral orbitofrontal gyrus R	2,4	0,4	2,6	0,3	−0,5	ns
Lateral orbitofrontal gyrus L	2,5	0,4	2,8	0,4	−0,7	ns
Gyrus rectus R	1,5	0,2	1,6	0,2	−0,4	ns
Gyrus rectus L	1,5	0,2	1,5	0,2	−0,4	ns
Postcentral gyrus R	6,4	0,9	6,9	0,9	−0,5	ns
Postcentral gyrus L	7,1	1,1	7,6	1,0	−0,4	ns
Superior parietal gyrus R	10,0	1,4	11,1	1,3	−0,8	0.01
Superior parietal gyrus L	10,2	1,3	11,0	1,3	−0,6	ns
Supramarginal gyrus R	6,5	1,1	6,9	0,9	−0,5	ns

(*continued on next page*)

Table 5 (*continued*)

	Gray matter Patients		*C9orf72* negative ALS		z scores	p-values
	Mean	SD	Mean	SD		
Supramarginal gyrus L	7,1	1,1	7,8	0,9	−0,8	0.04
Angular gyrus R	9,3	1,1	10,1	1,1	−0,7	0.03
Angular gyrus L	8,6	1,2	9,6	1,0	−1,0	<0.001
Precuneus R	5,6	0,6	6,1	0,6	−0,8	0.01
Precuneus L	5,6	0,6	6,0	0,7	−0,6	ns
Superior occipital gyrus R	3,0	0,5	3,4	0,6	−0,6	ns
Superior occipital gyrus L	2,7	0,5	3,1	0,5	−0,7	0.02
Middle occipital gyrus R	9,2	1,2	10,1	1,3	−0,7	<0.05
Middle occipital gyrus L	8,6	1,1	9,7	1,2	−0,9	<0.001
Inferior occipital gyrus R	5,3	0,7	5,5	0,7	−0,3	ns
Inferior occipital gyrus L	5,4	0,7	5,7	0,7	−0,4	ns
Cuneus R	3,1	0,5	3,3	0,6	−0,4	ns
Cuneus L	2,2	0,5	2,4	0,5	−0,5	ns
Superior temporal gyrus R	14,0	2,1	14,6	1,9	−0,4	ns
Superior temporal gyrus L	15,9	2,3	16,7	1,8	−0,5	ns
Middle temporal gyrus R	12,7	1,4	13,4	1,4	−0,4	ns
Middle temporal gyrus L	12,6	1,4	13,6	1,4	−0,8	0.03
Inferior temporal gyrus R	11,4	1,1	11,6	1,3	−0,2	ns
Inferior temporal gyrus L	11,1	1,3	11,6	1,1	−0,4	ns
Parahippocampal gyrus R	4,2	0,5	4,2	0,5	−0,1	ns
Parahippocampal gyrus L	3,8	0,5	3,8	0,4	−0,2	ns
Lingual gyrus R	8,1	1,1	8,6	1,0	−0,4	ns
Lingual gyrus L	7,5	1,0	7,9	1,0	−0,4	ns
Fusiform gyrus R	7,3	0,8	7,5	0,8	−0,3	ns
Fusiform gyrus L	7,6	0,8	7,8	0,7	−0,4	ns
Cingulate gyrus R	7,5	0,8	7,8	0,9	−0,3	ns
Cingulate gyrus L	7,6	0,9	7,9	0,9	−0,4	ns

Table 6
Correlations between DTI-based ROI analysis of frontal lobes, corticospinal tracts and ECAS.

ECAS	frontal lobes		upper corticospinal tract (CST)		lower corticospinal tract (CST)	
	Spearman r	p-value	Spearman r	p-value	Spearman r	p-value
language	0.40	**0.03**	−0.15	1.0	0.10	1.0
verbal fluency	0.34	**0.04**	−0.03	1.0	0.28	0.59
executive functions	0.45	**0.02**	−0.04	1.0	0.09	1.0
ALS specific score	0.53	**0.003**	−0.10	1.0	0.21	1.0
memory	0.36	**0.04**	−0.06	1.0	−0.02	1.0
spatial perception	0.52	**0.003**	0.06	1.0	0.20	1.0
Non ALS specific score	0.42	**0.03**	−0.06	1.0	0.02	1.0
Total score	0.50	**0.001**	−0.13	1.0	0.18	1.0

All p-values were adjusted with Bonferroni-Holm equation for multiple testing. ALS: Amyotrophic lateral sclerosis, CST: corticospinal tract, DTI: diffusion tensor-imaging, ECAS: Edinburgh Cognitive and Behavioral ALS Screen, Spearman r: Spearman correlation coefficient, ROI: region of interest.

aggravation across lifespan (Lee et al., 2017). Cortical thinning in frontal, temporal and parietal lobes in presymptomatic *C9orf72* gene carriers, decades before the development of first symptoms, have been also reported in a study analyzing cerebral alterations in patients with FTD (Le Blanc et al., 2020). Our findings - in addition to our current understanding of *C9orf72* effects during the disease - may further support the concept of an additional effect of *C9orf72* mutations early in life, long before the TDP43-driven ALS pathology eventually derives.

In line with the pre-existing literature, we could demonstrate that volume reduction in *C9orf72* ALS patients compared to *C9orf72* negative ALS is prominent in the thalamus as a multimodal integration relay area. In this context, lower volumes of the thalamus have been reported in ALS patients with *C9orf72* mutations, as well as in patients with ALS-FTD and FTD (Agosta et al., 2017; Bocchetta et al., 2018; Nigri et al., 2023; Schönecker et al., 2018; van der Burgh et al., 2020; Westeneng et al. 2016). Alterations in subcortical gray matter of the thalamus and the hippocampus were recently reported to occur in presymptomatic *C9orf72* gene carriers and to precede changes in cortical gray matter (Bede et al., 2023).

There are previous MRI based studies discussing the question of a characteristic MRI signature of ALS patients with *C9orf72* mutations, in part with heterogeneous results (Agosta et al., 2017; Bede et al., 2018; Chipika et al., 2020; Floeter and Gendron, 2018; Häkkinen et al., 2020; Li Hi Shing et al., 2021; Omer et al., 2017; van der Burgh et al., 2020; Westeneng et al., 2016). Westeneng et al. (n = 14) reported cortical atrophy in the opercular, fusiform, lingual, isthmus-cingulate and superior parietal cortex to be typical for these patients (Westeneng et al., 2016). In contrast, Agosta et al. (n = 19) described posterior cortical, cerebellar and thalamic alterations in brain MRI as characteristic for *C9orf72* ALS patients, whereas additional frontotemporal cortical and widespread alterations of white matter where seen as an effect of disease evolution (Agosta et al., 2017). Van der Burgh et al. (n = 24) described more extensive cortical and subcortical alterations with involvement of bilateral thalami, basal ganglia, hippocampi and amygdala in ALS patients with *C9orf72* mutations (van der Burgh et al., 2020). Nigri et al. (n = 24) reported a characteristic thalamo-cortico-striatal atrophy in *C9orf72* ALS patients compared to sporadic controls (Nigri et al., 2023). In our study, distinct reductions of whole cerebral gray matter volume and in the thalamus, as well as FA reductions in the frontal lobes and in the corticospinal tracts were shown already shortly after the development of first symptoms. Thus, these ubiquitous changes may be regarded as characteristics of *C9orf72*-associated ALS. However, we observed a peak of cortical volume reductions in frontal structures as an indicator of early frontal involvement in *C9orf72*-associated ALS. An overlap

between clinical, genetic and pathological features (Häkkinen et al., 2020), but also of neurostructural alterations of gray and white matter detected in neuroimaging (Crespi et al., 2018) in patients with ALS and FTD led to the hypothesis of the FTD-ALS continuum. Overlapping clinical symptoms of FTD are especially reported to be more frequent in ALS patients carrying *C9orf72* mutations as compared to patients without causative gene mutations or *SOD1*, respectively (Wiesenfarth et al., 2023; Mandrioli et al., 2022). In the current study, correlations between structural alterations and neuropsychological results in ECAS were specifically observed for association fibers projecting to the frontal lobes, i.e., lower FA values in the frontal lobes were associated with statistically significantly worse performance in all ECAS domains. The frontal cortex is known to be essential to perform these cognitive tasks (Lulé et al., 2018) so the presented pattern is in line with the proposed disease pathology.

Although we showed a generalized volume reduction in cerebral gray matter in ALS patients with *C9orf72* mutations compared to healthy controls and *C9orf72* negative ALS patients, respectively, significant negative correlations with clinical features existed between gray matter and age of onset. The negative correlation between FA values of gray matter and age of onset can be explained by the fact that *C9orf72* patients had lower age-related FA values. Interestingly, correlations were not only found between cognitive performance in ECAS and volumetric results of whole brain, cerebrum, gray matter of bilateral middle frontal, right superior parietal cortex and left supramarginal gyrus, but also of the basal ganglia (striatum, caudate, accumbens) and regions of the midbrain. These results can be regarded as compatible with the findings that basal ganglia are involved in the development of neuropsychological deficits in ALS (Machts et al., 2015), and strengthen the hypothesis of an functional alteration in the thalamo-cortico-striatal circuit in *C9orf72* ALS patients (Nigri et al., 2023). In a study analyzing presymptomatic *C9orf72* gene carriers, no correlations between neuropsychological scores and structural or microstructural alterations were found (Bertrand et al., 2018). Of note, in a previous study, we could not detect a *C9orf72*-specific pattern of neuropsychological deficits in ALS patients, although *C9orf72* ALS patients obtained worse ECAS results compared to *SOD1* and sporadic patients (Wiesenfarth et al., 2023).

In addition to the detection of structural changes, neuroimaging has been applied to investigate metabolic alterations in ALS patients with *C9orf72* mutations by the use of ^{18}F-2-fluoro-2-deoxy-D-glucose positron emission tomography (FDG PET). The findings of Cistaro et al. with widespread hypometabolism in *C9orf72*-associated ALS, including the limbic system as well as the caudate and thalamus and frontal regions - if FTD symptoms are present - (Cistaro et al., 2014) are in line with the volume reduction in these regions in our study. The same applies to reduced glucose metabolism in the *peri*-rolandic region, the precuneus, and the thalamus as shown by De Vocht et al. (De Vocht et al., 2023).

The findings should be considered in the context of certain strengths, but also some limitations. Due to the retrospective design, data of neuropsychological examination were not available for all patients and MRI was not performed at a standardized time after diagnosis or development of first symptoms - yet, in *C9orf72* ALS patients with a median delay of 11 months after onset of disease and 8.5 days after diagnosis still in an early stage of the disease. However, the retrospective approach allowed us to study one of the largest groups of *C9orf72*-associated ALS patients to date. All patients were clinically well described by physicians with dedicated experience in the diagnosis of ALS (motor neuron disease specialists). A limitation of the study was that p-NfH levels in CSF were not available in *C9orf72*-negative ALS patients. To overcome the limitations of heterogeneous assessment of clinical data at different times after the onset of the disease, a prospective study would be necessary. However, *C9orf72* as a genetic cause of ALS was first described in 2011 (DeJesus-Hernandez et al., 2011; Renton et al., 2011) and has been regularly tested in patients with negative family history only in recent years. Since it was shown that *C9orf72* mutations often also occur in apparently sporadic cases (Wiesenfarth et al., 2023) and targeted therapeutic strategies like the application of transposons or intrathecal ASO are currently being developed, genetic variants move into focus. In the future, it will be possible to perform prospective studies with sufficient number of cases.

To the best of our knowledge, for the first time, advanced unbiased imaging analysis of gray and white matter alterations in a multiparametric approach including ABV and DTI, comparison of results with *C9orf72*-negative ALS patients and healthy controls, and correlation analysis with clinical and neuropsychometric data have been integrated in one study with a large cohort size of more than 50 *C9orf72* ALS patients. Therefore, in addition to the validation of the results in the previous literature (Westeneng et al., 2016; Agosta et al., 2017; Bede et al., 2018; Omer et al., 2017; van der Burgh et al., 2020), our study was able to generate new findings. Due to a more aggressive disease course and cognitive decline, in comparison to *C9orf72* negative ALS, a special focus was placed on frontal involvement. One special strength is that our analysis was not limited to assessment of morphological gray matter and white matter structure together with structural connectivity alterations in MRI, but also included an evaluation of possible correlations between the MRI alterations and a large number of clinical, neuropsychometric, genetic, and CSF diagnostic parameters.

5. Conclusion

In conclusion, the results of our study, summarized in brief as the ubiquitous volume reduction of gray matter structures with frontal and parietal predominance together with reduced microstructure both in the corticospinal tracts and fibers projecting to the frontal lobes versus controls (including significant correlations to performance in ECAS) and frontally also versus *C9orf72* negative ALS patients, strengthen the hypothesis that an underlying developmental disorder in these patients leads to a more severe form of disease. Therefore, generalized volume reduction of whole cerebral gray matter and the thalamus seems to be one typical MRI feature of *C9orf72* ALS, together with bilateral alterations in axonal white matter structures to the frontal lobes. These data further support MRI as an appropriate *in vivo* biomarker even in the early phase of *C9orf72* ALS.

CRediT authorship contribution statement

Maximilian Wiesenfarth: Formal analysis, Investigation, Visualization, Writing – original draft. **Hans-Jürgen Huppertz:** Software, Formal analysis, Visualization, Investigation, Writing – review & editing. **Johannes Dorst:** Investigation, Writing – review & editing. **Dorothée Lulé:** Investigation, Writing – review & editing. **Albert C. Ludolph:** Investigation, Supervision, Writing – review & editing. **Hans-Peter Müller:** Conceptualization, Methodology, Software, Formal analysis, Visualization, Investigation, Supervision, Writing – original draft. **Jan Kassubek:** Conceptualization, Methodology, Visualization, Investigation, Supervision, Writing – original draft, Project administration.

Declaration of Competing Interest

The authors declare that they have no known competing financial interests or personal relationships that could have appeared to influence the work reported in this paper.

Data availability

Data will be made available on request.

Acknowledgements

Kornelia Günther is gratefully acknowledged for her help in assembling the clinical data.

Appendix A. Supplementary data

Supplementary data to this article can be found online at https://doi.org/10.1016/j.nicl.2023.103505.

References

Abrahams, S., Newton, J., Niven, E., Foley, J., Bak, T.H., 2014. Screening for cognition and behaviour changes in ALS. Amyotroph Lateral Scler Frontotemporal Degener 15 (1–2), 9–14. https://doi.org/10.3109/21678421.2013.805784.

Agosta, F., Ferraro, P.M., Riva, N., Spinelli, E.G., Domi, T., Carrera, P., Copetti, M., Falzone, Y., Ferrari, M., Lunetta, C., Comi, G., Falini, A., Quattrini, A., Filippi, M., 2017. Structural and functional brain signatures of C9orf72 in motor neuron disease. Neurobiol. Aging 57, 206–219.

Balendra, R., Isaacs, A.M., 2018. C9orf72-mediated ALS and FTD: multiple pathways to disease. Nat. Rev. Neurol. 14 (9), 544–558. https://doi.org/10.1038/s41582-018-0047-2.

Bede, P., Bokde, A.L.W., Byrne, S., Elamin, M., McLaughlin, R.L., Kenna, K., Fagan, A.J., Pender, N., Bradley, D.G., Hardiman, O., 2013. Multiparametric MRI study of ALS stratified for the C9orf72 genotype. Neurology 81 (4), 361–369.

Bede, P., Omer, T., Finegan, E., Chipika, R.H., Iyer, P.M., Doherty, M.A., Vajda, A., Pender, N., McLaughlin, R.L., Hutchinson, S., Hardiman, O., 2018. Connectivity-based characterisation of subcortical grey matter pathology in frontotemporal dementia and ALS: a multimodal neuroimaging study. Brain Imaging Behav. 12 (6), 1696–1707.

Bede, P., Lulé, D., Müller, H.-P., Tan, E.L., Dorst, J., Ludolph, A.C., Kassubek, J., 2023. Presymptomatic grey matter alterations in ALS kindreds: a computational neuroimaging study of asymptomatic C9orf72 and SOD1 mutation carriers. J. Neurol. 270 (9), 4235–4247.

Benatar, M., Zhang, L., Wang, L., Granit, V., Statland, J., Barohn, R., Swenson, A., Ravits, J., Jackson, C., Burns, T.M., Trivedi, J., Pioro, E.P., Caress, J., Katz, J., McCauley, J.L., Rademakers, R., Malaspina, A., Ostrow, L.W., Wuu, J., 2020. Validation of serum neurofilaments as prognostic and potential pharmacodynamic biomarkers for ALS. Neurology 95 (1), e59–e69.

Bertrand, A., Wen, J., Rinaldi, D., Houot, M., Sayah, S., Camuzat, A., Fournier, C., Fontanella, S., Routier, A., Couratier, P., Pasquier, F., Habert, M.-O., Hannequin, D., Martinaud, O., Caroppo, P., Levy, R., Dubois, B., Brice, A., Durrleman, S., Colliot, O., Le Ber, I., 2018. Early Cognitive, Structural, and Microstructural Changes in Presymptomatic C9orf72 Carriers Younger Than 40 Years. JAMA Neurol. 75 (2), 236.

Bocchetta, M., Gordon, E., Cardoso, M.J., et al., 2018. Thalamic atrophy in frontotemporal dementia - Not just a C9orf72 problem. Neuroimage Clin. 18, 675–681. https://doi.org/10.1016/j.nicl.2018.02.019. Published 2018 Feb 23.

Braak, H., Brettschneider, J., Ludolph, A.C., Lee, V.M., Trojanowski, J.Q., Del Tredici, K., 2013. Amyotrophic lateral sclerosis–a model of corticofugal axonal spread. Nat. Rev. Neurol. 9 (12), 708–714. https://doi.org/10.1038/nrneurol.2013.221.

Brenner, D., Freischmidt, A., 2022. Update on genetics of amyotrophic lateral sclerosis. Curr. Opin. Neurol. 35 (5), 672–677. https://doi.org/10.1097/WCO.0000000000001093.

Brettschneider, J., Del Tredici, K., Toledo, J.B., Robinson, J.L., Irwin, D.J., Grossman, M., Suh, EunRan, Van Deerlin, V.M., Wood, E.M., Baek, Y., Kwong, L., Lee, E.B., Elman, L., McCluskey, L., Fang, L., Feldengut, S., Ludolph, A.C., Lee, V.-Y., Braak, H., Trojanowski, J.Q., 2013. Stages of pTDP-43 pathology in amyotrophic lateral sclerosis. Ann. Neurol. 74 (1), 20–38.

Brettschneider, J., Del Tredici, K., Lee, V.M., Trojanowski, J.Q., 2015. Spreading of pathology in neurodegenerative diseases: a focus on human studies. Nat. Rev. Neurosci. 16 (2), 109–120. https://doi.org/10.1038/nrn3887.

Byrne, S., Elamin, M., Bede, P., Shatunov, A., Walsh, C., Corr, B., Heverin, M., Jordan, N., Kenna, K., Lynch, C., McLaughlin, R.L., Iyer, P.M., O'Brien, C., Phukan, J., Wynne, B., Bokde, A.L., Bradley, D.G., Pender, N., Al-Chalabi, A., Hardiman, O., 2012. Cognitive and clinical characteristics of patients with amyotrophic lateral sclerosis carrying a C9orf72 repeat expansion: a population-based cohort study. Lancet Neurol. 11 (3), 232–240.

Cedarbaum, J.M., Stambler, N., Malta, E., Fuller, C., Hilt, D., Thurmond, B., Nakanishi, A., 1999. The ALSFRS-R: a revised ALS functional rating scale that incorporates assessments of respiratory function. BDNF ALS Study Group (Phase III). J. Neurol. Sci. 169 (1-2), 13–21.

Chipika, R.H., Siah, W.F., Shing, S.L.H., Finegan, E., McKenna, M.C., Christidi, F., Chang, K.M., Karavasilis, E., Vajda, A., Hengeveld, J.C., Doherty, M.A., Donaghy, C., Hutchinson, S., McLaughlin, R.L., Hardiman, O., Bede, P., 2020. MRI data confirm the selective involvement of thalamic and amygdalar nuclei in amyotrophic lateral sclerosis and primary lateral sclerosis. Data Brief 32, 106246.

Cistaro, A., Pagani, M., Montuschi, A., Calvo, A., Moglia, C., Canosa, A., Restagno, G., Brunetti, M., Traynor, B.J., Nobili, F., Carrara, G., Fania, P., Lopiano, L., Valentini, M.C., Chiò, A., 2014. The metabolic signature of C9orf72-related ALS: FDG PET comparison with nonmutated patients. Eur. J. Nucl. Med. Mol. Imaging 41 (5), 844–852.

Crespi, C., Dodich, A., Cappa, S.F., Canessa, N., Iannaccone, S., Corbo, M., Lunetta, C., Falini, A., Cerami, C., 2018. Multimodal MRI quantification of the common neurostructural bases within the FTD-ALS continuum. Neurobiol. Aging 62, 95–104.

De Vocht, J., Van Weehaeghe, D., Ombelet, F., et al., 2023. Differences in Cerebral Glucose Metabolism in ALS Patients with and without C9orf72 and SOD1 Mutations. Cells 12 (6), 933. https://doi.org/10.3390/cells12060933.

DeJesus-Hernandez, M., Mackenzie, I., Boeve, B., Boxer, A., Baker, M., Rutherford, N., Nicholson, A., Finch, NiColeA., Flynn, H., Adamson, J., Kouri, N., Wojtas, A., Sengdy, P., Hsiung, G.-Y., Karydas, A., Seeley, W., Josephs, K., Coppola, G., Geschwind, D., Wszolek, Z., Feldman, H., Knopman, D., Petersen, R., Miller, B., Dickson, D., Boylan, K., Graff-Radford, N., Rademakers, R., 2011. Expanded GGGGCC hexanucleotide repeat in noncoding region of C9ORF72 causes chromosome 9p-linked FTD and ALS. Neuron 72 (2), 245–256.

Dreger, M., Steinbach, R., Otto, M., Turner, M.R., Grosskreutz, J., 2022. Cerebrospinal fluid biomarkers of disease activity and progression in amyotrophic lateral sclerosis. J. Neurol. Neurosurg. Psychiatry 93 (4), 422–435. https://doi.org/10.1136/jnnp-2021-327503.

Feldman, E.L., Goutman, S.A., Petri, S., Mazzini, L., Savelieff, M.G., Shaw, P.J., Sobue, G., 2022. Amyotrophic lateral sclerosis. Lancet 400 (10360), 1363–1380.

Floeter, M.K., Gendron, T.F., 2018. Biomarkers for Amyotrophic Lateral Sclerosis and Frontotemporal Dementia Associated With Hexanucleotide Expansion Mutations in C9orf72. Front. Neurol. 9, 1063. https://doi.org/10.3389/fneur.2018.01063.

Frings, L., Mader, I., Landwehrmeyer, B.G., Weiller, C., Hüll, M., Huppertz, H.J., 2012. Quantifying change in individual subjects affected by frontotemporal lobar degeneration using automated longitudinal MRI volumetry. Hum. Brain Mapp. 33 (7), 1526–1535. https://doi.org/10.1002/hbm.21304.

Gagliardi, D., Faravelli, I., Meneri, M., Saccomanno, D., Govoni, A., Magri, F., Ricci, G., Siciliano, G., Pietro Comi, G., Corti, S., 2021. Diagnostic and prognostic value of CSF neurofilaments in a cohort of patients with motor neuron disease: A cross-sectional study. J. Cell Mol. Med. 25 (8), 3765–3771.

Gendron, T.F., Daughrity, L.M., Heckman, M.G., Diehl, N.N., Wuu, J., Miller, T.M., Pastor, P., Trojanowski, J.Q., Grossman, M., Berry, J.D., Hu, W.T., Ratti, A., Benatar, M., Silani, V., Glass, J.D., Floeter, M.K., Jeromin, A., Boylan, K.B., Petrucelli, L., 2017. Phosphorylated neurofilament heavy chain: A biomarker of survival for C9ORF72-associated amyotrophic lateral sclerosis. Ann. Neurol. 82 (1), 139–146.

Häkkinen, S., Chu, S.A., Lee, S.E., 2020. Neuroimaging in genetic frontotemporal dementia and amyotrophic lateral sclerosis. Neurobiol. Dis. 145, 105063 https://doi.org/10.1016/j.nbd.2020.105063.

Höglinger, G.U., Huppertz, H.-J., Wagenpfeil, S., Andrés, M.V., Belloch, V., León, T., del Ser, T., 2014. Tideglusib reduces progression of brain atrophy in progressive supranuclear palsy in a randomized trial. Mov. Disord. 29 (4), 479–487.

Hübers, A., Marroquin, N., Schmoll, B., Vielhaber, S., Just, M., Mayer, B., Högel, J., Dorst, J., Mertens, T., Just, W., Aulitzky, A., Wais, V., Ludolph, A.C., Kubisch, C., Weishaupt, J.H., Volk, A.E., 2014. Polymerase chain reaction and Southern blot-based analysis of the C9orf72 hexanucleotide repeat in different motor neuron diseases. Neurobiol. Aging 35 (5), 1214.

Huppertz, H.-J., Möller, L., Südmeyer, M., Hilker, R., Hattingen, E., Egger, K., Amtage, F., Respondek, G., Stamelou, M., Schnitzler, A., Pinkhardt, E.H., Oertel, W.H., Knake, S., Kassubek, J., Höglinger, G.U., 2016. Differentiation of neurodegenerative parkinsonian syndromes by volumetric magnetic resonance imaging analysis and support vector machine classification. Mov. Disord. 31 (10), 1506–1517.

Kalra, S., Müller, H.-P., Ishaque, A., Zinman, L., Korngut, L., Genge, A., Beaulieu, C., Frayne, R., Graham, S.J., Kassubek, J., 2020. A prospective harmonized multicenter DTI study of cerebral white matter degeneration in ALS. Neurology 95 (8), e943–e952.

Kassubek, J., Pinkhardt, E.H., Dietmaier, A., Ludolph, A.C., Landwehrmeyer, G.B., Huppertz, H.J., 2011. Fully automated atlas-based MR imaging volumetry in Huntington disease, compared with manual volumetry. AJNR Am. J. Neuroradiol. 32 (7), 1328–1332. https://doi.org/10.3174/ajnr.A2514.

Kassubek, J., Müller, H.-P., Del Tredici, K., Lulé, D., Gorges, M., Braak, H., Ludolph, A.C., 2018. Imaging the pathoanatomy of amyotrophic lateral sclerosis in vivo: targeting a propagation-based biological marker. J. Neurol. Neurosurg. Psychiatry 89 (4), 374–381.

Khalil, M., Teunissen, C.E., Otto, M., Piehl, F., Sormani, M.P., Gattringer, T., Barro, C., Kappos, L., Comabella, M., Fazekas, F., Petzold, A., Blennow, K., Zetterberg, H., Kuhle, J., 2018. Neurofilaments as biomarkers in neurological disorders. Nat. Rev. Neurol. 14 (10), 577–589.

Le Blanc, G., Jetté Pomerleau, V., McCarthy, J., et al., 2020. Faster Cortical Thinning and Surface Area Loss in Presymptomatic and Symptomatic C9orf72 Repeat Expansion Adult Carriers. Ann. Neurol. 88 (1), 113–122. https://doi.org/10.1002/ana.25748.

Lee SE, Sias AC, Mandelli ML, et al. Network degeneration and dysfunction in presymptomatic *C9ORF72* expansion carriers. *Neuroimage Clin.* 2017;14:286-297. Published 2016 Dec 10. 10.1016/j.nicl.2016.12.006.

Lee, E.B., Lee, V.-Y., Trojanowski, J.Q., 2011. Gains or losses: molecular mechanisms of TDP43-mediated neurodegeneration. Nat. Rev. Neurosci. 13 (1), 38–50.

Li Hi Shing, S., McKenna, M.C., Siah, W.F., Chipika, R.H., Hardiman, O., Bede, P., 2021. The imaging signature of C9orf72 hexanucleotide repeat expansions: implications for clinical trials and therapy development. Brain Imaging Behav. 15 (5), 2693–2719. https://doi.org/10.1007/s11682-020-00429-w.

Loose, M., Burkhardt, C., Aho-Özhan, H., Keller, J., Abdulla, S., Böhm, S., Kollewe, K., Uttner, I., Abrahams, S., Petri, S., Weber, M., Ludolph, A.C., Lulé, D., 2016. Age and education-matched cut-off scores for the revised German/Swiss-German version of ECAS. Amyotroph Lateral Scler Frontotemporal Degener 17 (5-6), 374–376.

Ludolph, A., Drory, V., Hardiman, O., Nakano, I., Ravits, J., Robberecht, W., Shefner, J., 2015. A revision of the El Escorial criteria - 2015. Amyotroph Lateral Scler Frontotemporal Degener 16 (5-6), 291–292.

Lulé, D., Burkhardt, C., Abdulla, S., Böhm, S., Kollewe, K., Uttner, I., Abrahams, S., Bak, T.H., Petri, S., Weber, M., Ludolph, A.C., 2015. The Edinburgh Cognitive and Behavioural Amyotrophic Lateral Sclerosis Screen: a cross-sectional comparison of established screening tools in a German-Swiss population. Amyotroph Lateral Scler Frontotemporal Degener 16 (1-2), 16–23.

Lulé, D., Böhm, S., Müller, H.-P., Aho-Özhan, H., Keller, J., Gorges, M., Loose, M., Weishaupt, J.H., Uttner, I., Pinkhardt, E., Kassubek, J., Del Tredici, K., Braak, H., Abrahams, S., Ludolph, A.C., 2018. Cognitive phenotypes of sequential staging in amyotrophic lateral sclerosis. Cortex 101, 163–171.

Lulé, D.E., Müller, H.P., Finsel, J., et al., 2020. Deficits in verbal fluency in presymptomatic C9orf72 mutation gene carriers-a developmental disorder. J. Neurol. Neurosurg. Psychiatry 91 (11), 1195–1200. https://doi.org/10.1136/jnnp-2020-323671.

Machts, J., Loewe, K., Kaufmann, J., Jakubiczka, S., Abdulla, S., Petri, S., Dengler, R., Heinze, H.-J., Vielhaber, S., Schoenfeld, M.A., Bede, P., 2015. Basal ganglia pathology in ALS is associated with neuropsychological deficits. Neurology 85 (15), 1301–1309.

Mandrioli, J., Zucchi, E., Martinelli, I., Van der Most, L., Gianferrari, G., Moglia, C., Manera, U., Solero, L., Vasta, R., Canosa, A., Grassano, M., Brunetti, M., Mazzini, L., De Marchi, F., Simonini, C., Fini, N., Tupler, R., Vinceti, M., Chiò, A., Calvo, A., 2022. Factors predicting disease progression in C9ORF72 ALS patients. J. Neurol. 270 (2), 877–890.

Masrori, P., Van Damme, P., 2020. Amyotrophic lateral sclerosis: a clinical review. Eur. J. Neurol. 27 (10), 1918–1929. https://doi.org/10.1111/ene.14393.

Miller, T.M., Cudkowicz, M.E., Genge, A., et al., 2022. Trial of Antisense Oligonucleotide Tofersen for SOD1 ALS. New Engl. J. Med. 387 (12), 1099–1110. https://doi.org/10.1056/NEJMoa2204705.

Müller, K., Brenner, D., Weydt, P., Meyer, T., Grehl, T., Petri, S., Grosskreutz, J., Schuster, J., Volk, A.E., Borck, G., Kubisch, C., Klopstock, T., Zeller, D., Jablonka, S., Sendtner, M., Klebe, S., Knehr, A., Günther, K., Weis, J., Claeys, K.G., Schrank, B., Sperfeld, A.-D., Hübers, A., Otto, M., Dorst, J., Meitinger, T., Strom, T.M., Andersen, P.M., Ludolph, A.C., Weishaupt, J.H., 2018. Comprehensive analysis of the mutation spectrum in 301 German ALS families. J. Neurol. Neurosurg. Psychiatry 89 (8), 817–827.

Müller, H.-P., Del Tredici, K., Lulé, D., Müller, K., Weishaupt, J.H., Ludolph, A.C., Kassubek, J., 2020. *In vivo* histopathological staging in C9orf72-associated ALS: A tract of interest DTI study. Neuroimage Clin. 27, 102298.

Müller, H.P., Unrath, A., Ludolph, A.C., Kassubek, J., 2007. Preservation of diffusion tensor properties during spatial normalization by use of tensor imaging and fibre tracking on a normal brain database. Phys. Med. Biol. 52 (6), N99–N109. https://doi.org/10.1088/0031-9155/52/6/N01.

Müller, H.P., Lulé, D., Roselli, F., Behler, A., Ludolph, A.C., Kassubek, J., 2021. Segmental involvement of the corpus callosum in C9orf72-associated ALS: a tract of interest-based DTI study. Ther Adv. Chronic Dis. 12 https://doi.org/10.1177/20406223211002969.

Nigri, A., Umberto, M., Stanziano, M., Ferraro, S., Fedeli, D., Medina Carrion, J.P., Palermo, S., Lequio, L., Denegri, F., Agosta, F., Filippi, M., Valentini, M.C., Canosa, A., Calvo, A., Chiò, A., Bruzzone, M.G., Moglia, C., 2023. C9orf72 ALS mutation carriers show extensive cortical and subcortical damage compared to matched wild-type ALS patients. Neuroimage Clin. 38, 103400.

Omer, T., Finegan, E., Hutchinson, S., Doherty, M., Vajda, A., McLaughlin, R.L., Pender, N., Hardiman, O., Bede, P., 2017. Neuroimaging patterns along the ALS-FTD spectrum: a multiparametric imaging study. Amyotroph Lateral Scler Frontotemporal Degener 18 (7-8), 611–623.

Opfer, R., Suppa, P., Kepp, T., Spies, L., Schippling, S., Huppertz, H.-J., 2016. Atlas based brain volumetry: How to distinguish regional volume changes due to biological or physiological effects from inherent noise of the methodology. Magn. Reson. Imaging 34 (4), 455–461.

Rascovsky, K., Hodges, J.R., Knopman, D., et al., 2011. Sensitivity of revised diagnostic criteria for the behavioural variant of frontotemporal dementia. Brain 134 (Pt 9), 2456–2477. https://doi.org/10.1093/brain/awr179.

Renton, A.E., Majounie, E., Waite, A., et al., 2011. A hexanucleotide repeat expansion in C9ORF72 is the cause of chromosome 9p21-linked ALS-FTD. Neuron 72 (2), 257–268. https://doi.org/10.1016/j.neuron.2011.09.010.

Schönecker, S., Neuhofer, C., Otto, M., et al., 2018. Atrophy in the Thalamus But Not Cerebellum Is Specific for C9orf72 FTD and ALS Patients - An Atlas-Based Volumetric MRI Study. Front. Aging Neurosci. 10, 45. https://doi.org/10.3389/fnagi.2018.00045.

Steinacker P, Feneberg E, Weishaupt J, et al. Neurofilaments in the diagnosis of motoneuron diseases: a prospective study on 455 patients. *J. Neurol. Neurosurg. Psychiatry*. 2016;87(1):12-20. 10.1136/jnnp-2015-311387.

Umoh, M.E., Fournier, C., Li, Y., et al., 2016. Comparative analysis of C9orf72 and sporadic disease in an ALS clinic population. Neurology 87 (10), 1024–1030. https://doi.org/10.1212/WNL.0000000000003067.

van der Burgh, H.K., Westeneng, H.-J., Walhout, R., van Veenhuijzen, K., Tan, H.H.G., Meier, J.M., Bakker, L.A., Hendrikse, J., van Es, M.A., Veldink, J.H., van den Heuvel, M.P., van den Berg, L.H., 2020. Multimodal longitudinal study of structural brain involvement in amyotrophic lateral sclerosis. Neurology 94 (24), e2592–e2604.

Westeneng, H.-J., Walhout, R., Straathof, M., Schmidt, R., Hendrikse, J., Veldink, J.H., van den Heuvel, M.P., van den Berg, L.H., 2016. Widespread structural brain involvement in ALS is not limited to the C9orf72 repeat expansion. J. Neurol. Neurosurg. Psychiatry 87 (12), 1354–1360.

Wiesenfarth M, Günther K, Müller K, et al. Clinical and genetic features of amyotrophic lateral sclerosis patients with *C9orf72* mutations. *Brain Commun.* Brain Commun. 2023;5(2):fcad087. 10.1093/braincomms/fcad087.

Yeh, T.-H., Liu, H.-F., Li, Y.-W., Lu, C.-S., Shih, H.-Y., Chiu, C.-C., Lin, S.-J., Huang, Y.-C., Cheng, Y.-C., 2018. C9orf72 is essential for neurodevelopment and motility mediated by Cyclin G1. Exp. Neurol. 304, 114–124.